Trop J Nat Prod Res, October 2025; 9(10): 5061 - 5072
ISSN 2616-0684 (Print)
ISSN 2616-0692 (Electronic)

Tropical Journal of Natural Product Research

Available online at https://www.tjnpr.org

Original Research Article

Exploring the Protein Targets of *Cinnamomum zeylanicum*'s Phytoconstituents Against Pathogenic *Staphylococcus aureus*: GC-MS Profiling, Molecular Docking, Pharmacophore Modeling, and Pathway Analysis

Sarit Prabha*, Sudeesh Warkare, Akash Ranga, Khushhali M. Pandey

Center for Genomics Lab, Department of Biological Science and Engineering, Maulana Azad National Institute of Technology, Bhopal, India

ARTICLE INFO

Article history:
Received 02 September 2025
Revised 06 October 2025
Accepted 08 October 2025
Published online 01 November 2025

ABSTRACT

Staphylococcus aureus is a major cause of severe infections, including sepsis, largely due to its diverse virulence factors and increasing antibiotic resistance, which highlights the need for alternative therapeutic strategies. The traditional medicinal plant, *Cinnamomum zeylanicum*, has rich bioactive secondary metabolites. In this study, we investigated the antimicrobial potential of *C. zeylanicum* bark against pathogenic *S. aureus* through minimum inhibitory and bactericidal concentration assays, along with phytoconstituent profiling using GC-MS. Virulence factors of *S. aureus* were characterized by PCR targeting the plc, icaA, and nuc genes. The identified phytoconstituents were further analyzed *in silico*, including molecular docking, pharmacophore modeling, and ADMET analysis against *S. aureus* target proteins. A tetrapartite interaction network and pathway analysis were constructed using STRING and KEGG databases. The methanol extract, containing 19 phytoconstituents, exhibited significant antibacterial activity with MIC and MBC values of 5 mg/mL. Docking results revealed that α-copaene, α-muurolene, and τ-cadinol showed strong binding interactions with D-alanine-D-alanine ligase, dihydrofolate reductase, peptide deformylase, and penicillin-binding protein 2a. These findings suggest that *C. zeylanicum* bark extract, enriched with phenolic and flavonoid derivatives, holds promise as a natural source of anti-*S. aureus* agents. However, further experimental validation is needed to confirm the predicted protein targets and pathways.

Keywords: *Cinnamomum zeylanicum*, *Staphylococcus aureus*, Gas Chromatography Mass Spectrometer, Molecular docking, Pathway analysis

Introduction

The pathogenesis of bacterial infections plays a critical role in the prognosis of diseases such as sepsis, which can be caused by various bacteria, including *Staphylococcus aureus* (*S. aureus*), *Pseudomonas aeruginosa*, *Escherichia coli*, *Klebsiella pneumoniae*, and *Streptococcus pneumoniae*.[1] Among these, *S. aureus* is a gram-positive bacterium, a leading cause of infection, and is frequently associated with illness and a high mortality rate. The bacterium is commonly present on skin, mucosa, bones, and joints. The clinical challenge arises because diverse bacterial virulence factors and the capacity to develop multidrug resistance are also emphasized by the World Health Organization in 2018.[2–4] Virulence factors such as beta-haemolysin (β-hlb), thermonuclease (nuc), and immune evasion strategies such as polysaccharide intercellular adhesion (PIA) play a critical role in pathogenesis by disrupting the human immune response. β-hlb activates the epidermal growth factor receptor, enhancing skin colonization and inflammation,[5,6] while nuc and PIA promote biofilm formation through adhesion and aggregation.[7–9]

*Corresponding author. E mail: saritprabha32@gmail.com
Tel: (+91) 7355648221

Citation: Prabha S, Warkare S, Ranga A, Pandey KM. Exploring the Protein Targets of *Cinnamomum zeylanicum*'s Phytoconstituents Against Pathogenic *Staphylococcus aureus*: GC-MS Profiling, Molecular Docking, Pharmacophore Modeling, and Pathway Analysis. Trop J Nat Prod Res. 2025; 9(10): 5061 – 5072 https://doi.org/10.26538/tjnpr/v9i10.48

Official Journal of Natural Product Research Group, Faculty of Pharmacy, University of Benin, Benin City, Nigeria

Drug-resistant *S. aureus* exhibits resistance against cephalosporin, vancomycin, ceftazidime, daptomycin, and ciprofloxacin.[10] This alarming resistance trend highlights the need for alternative drugs. Ethnomedicinal plants have been recognized in traditional therapeutic systems and are known for their disease-preventive properties. *Cinnamomum zeylanicum* (family Lauraceae, *C. zeylanicum*) has a well-documented history of medicinal use and contains bioactive compounds such as cinnamaldehyde, eugenol, trans-cinnamaldehyde, cinnamic acid, and coumarin.[11–13] These compounds have been reported to exhibit diverse pharmacological activities, including antibacterial, anti-inflammatory, antioxidant, and anticancer effects.[14–18] Computational studies conducted by Mulpuru et al. and Meylani et al. have demonstrated that phytoconstituents of *C. zeylanicum* may inhibit the SARS-CoV-2 main protease and Candida species, respectively,[19,20] and Pourkhosravani et al. have highlighted the potential antibacterial activity of essential oil by targeting bacterial receptors.[21] However, the limited research studies have comprehensively profiled the phytochemical composition of *C. zeylanicum* bark and elucidated its interactions with specific bacterial targets.

The present study aims to identify the effective antibacterial phytoconstituents of *C. zeylanicum* against target proteins of *S. aureus* through a combined *in vitro* and *in silico* approach. *In vitro* analyses included phytoconstituent profiling through qualitative and quantitative evaluation, gas chromatography-mass spectrometry (GC-MS), and antimicrobial activity assays. *In silico* analyses involved molecular docking, pharmacophore modeling, and ADMET evaluation of identified phytoconstituents against validated *S. aureus* target proteins. Furthermore, protein-phytoconstituent interaction networks and metabolic pathways were analyzed using STRING and KEGG databases. This multidimensional approach provides a mechanistic understanding of the interactions between *C. zeylanicum* bark phytoconstituents and *S. aureus* target proteins, offering a foundation for the development of novel plant-based therapeutic agents.

 ISSN 2616-0684 (Print)
ISSN 2616-0692 (Electronic)

Materials and Methods

In vitro design

Plant collection and identification

Stem of *C. zeylanicum* bark (CzB) was collected in April 2024 from a market in Bhopal, India (23°14′06.5″N, 77°24′00.5″E). The sample was authenticated by a taxonomist at the Vedanta Testing & Research Laboratory, Bhopal, India, and a voucher number (1/19424R) was issued. The CzB was air-dried at 25°C for 5 days and ground to a coarse powder.

Extraction of plant material

The crude extract was prepared by maceration, where 40 g of powder was immersed in 150 mL of methanol (Loba Chemie, India) and shaken at 100 rpm for 5 days. The extract was filtered and concentrated under reduced pressure using a rotary evaporator (Heidolph, Germany) with a speed of 70 rpm and a temperature of 50°C. The extract was dried in an oven at 40°C to obtain the extract. Finally, yield (%) was calculated according to equation 1,[22] and the dried extract was stored at 4°C in an airtight container.

$$\text{Yield of CzB crude extract (\%)} = \frac{\text{weight of CzB crude extract}}{\text{total volume of solvent}} \times 100 \quad \ldots\ldots (1)$$

Qualitative and quantitative phytochemical screening

Qualitative phytochemical assays were performed to detect flavonoids, phenols, coumarins, alkaloids, and quinones.[23] The total phenolic content (TPC) was determined using the Folin-Ciocalteu method.[24] The extract (1 mg/mL) was mixed with diluted Folin-Ciocalteu reagent (2.5 mL, 1:10, Himedia, India) and sodium carbonate (3 mL, 7.5% w/v, Thermo Fisher Scientific, USA), incubated in the dark at 25 °C for 90 min, and absorbance measured at 750 nm (UV-Vis spectrophotometer, Thermo Fisher Scientific). Results were expressed as mg gallic acid equivalent/g extract (mg GAE/g). The total flavonoid content (TFC) was determined using the aluminum chloride colorimetric method.[25] The extract (1 mg/mL) was mixed with aluminum chloride (0.1 mL, Pallav, India), potassium acetate (0.1 mL, 1 M, Himedia, India), and distilled water (2.8 mL), incubated in the dark at 25 °C for 30 min, and the absorbance was measured at 510 nm. Results were expressed as mg quercetin equivalent/g extract (mg QE/g).

Gas chromatography mass spectrometer (GC-MS) profiling

GC-MS analysis was conducted using Shimadzu's GC-MS system with an Rxi-5Sil MS column. Helium was used as the carrier gas at 1 mL/min. The injector and detector temperatures were maintained at 250°C and 280°C, respectively. Oven temperature was programmed to increase at 10°C/min to 250°C (3 min hold), then ramped to 280°C at 30°C/min (2 min hold). Mass spectra were obtained in electron impact mode (70 eV).[26] The data were analyzed by ChemStation software version 14 and compared against the National Institute of Standards and Technology library.[27]

Genomic DNA extraction and molecular characterization of S. aureus

The freeze-dried culture of *S. aureus* MTCC 96 was obtained from the Microbial Type Culture Collection, Chandigarh, India. The bacterial culture was maintained on nutrient agar medium at 4°C, and the strain was revived in Luria-Bertani medium (Lennox, USA) and incubated at 37°C for 24 hours under sterile conditions. The culture density was standardized to the 0.5 McFarland standard, which is approximately 1.5 × 10^8 CFU/mL. Genomic DNA of *S. aureus* was extracted using the QIAamp® Genomic DNA Mini Kit, following the manufacturer's protocol. DNA quality was assessed by 2% agarose gel electrophoresis. Polymerase Chain Reaction (PCR) was used for molecular identification and characterization of *S. aureus* targeting 16S rRNA and virulence genes (nuc,[28] plc, and icaA) with gene-specific primers, respectively (table 1). Reactions were performed in a Thermal Cycler MJ Mini (BIO-RAD) using a Hi-PCR Kit (HiMedia, India). Amplification involved an initial denaturation at 95°C for 2 min, followed by 30 cycles of denaturation at 94°C for 1 min, annealing (54°C for 16S rRNA and plc, 50°C for icaA, and 55°C for nuc), and extension (72°C for 45 s, 1 min, and 1.5 min, respectively). A final extension was carried out at 72°C for 4 min, and products were visualized by 2% agarose gel electrophoresis.

Table 1: List of Primers used in the molecular characterization of *Staphylococcus aureus* MTCC96

Gene	ENA accession number	Primer	Sequence (5'- 3')	Amplicon size (bp)
icaA (N-acetyl-glucosaminyltransferase)	SUK09942.1	F	GAACCGCTTGCCATGTGTTG	497
		R	TTCCCTCTGTCTGGGCTTGA	
plc (phospholipase C)	SUJ92450.1	F	TGGGCAGATAACGCGACATT	284
		R	ATCAGCCAACCCGTTCTAG	
nuc [28] (thermostable nuclease)	SUJ96783.1	F	GCGATTGATGGTGATACGGTT	270
		R	ACGCAAGCCTTGACGAACTAAAGC	
16S rRNA	UHAE01000001.1	F	GAGTACGACCGCAAGGTTGA	204
		R	CCCAACATCTCACGACACGA	

Minimum inhibitory and bactericidal concentration

S. aureus colonies were incubated in Mueller-Hinton broth (HiMedia, India) at 37°C for 16-18 h, and cell density was adjusted to 5 × 10^5 CFU/mL by the McFarland method. The CzB extract was dissolved in 10% dimethyl sulfoxide (Finar, India), and ciprofloxacin was used as a positive control. Minimum inhibitory concentration (MIC) was determined by resazurin-based microdilution in 96-well plates incubated at 37 °C for 18 h, followed by the addition of resazurin dye (30 µL, 0.015%, Sulab, India) and further incubation for 3 h. The MIC was defined as the lowest concentration preventing a color change from blue to pink. Minimum bactericidal concentration (MBC) was determined by streaking wells onto Mueller-Hinton agar (HiMedia, India) and incubating at 37 °C for 18 h. The lowest concentration with no bacterial growth was recorded as the MBC.[29] All experiments were performed in triplicate, and results were analyzed by one-way ANOVA (Microsoft Excel 2016), with significance at $p < 0.05$.

In silico design

Proteins and phytoconstituents preparation

In our previous research,[30] seven potential drug target proteins of *S. aureus* were retrieved from the Protein Data Bank.[31] Only structures with resolution <2.0 Å were selected. Proteins were prepared in PDBQT format using AutoDock Tools version 1.5[32] by removing ligands, ions, and water molecules, adding missing atoms and polar hydrogens, and applying Kollman charges. The three-dimensional structure of the phytoconstituents of CzB, identified through GC-MS analysis, was prepared using MarvinSketch version 3.0[33] and then optimized with the MMFF94 force field. Then, structures were saved in SDF format and converted to PDBQT using OpenBabel version 3.1.[34]

 ISSN 2616-0684 (Print)
ISSN 2616-0692 (Electronic)

Molecular docking, principal component analysis, and pharmacophore modeling

Molecular docking was performed using AutoDock Vina (ADV) version 1.1.[32] Grid parameters were taken from previous studies, and docking configuration files were executed via Perl scripts. Docked complexes were visualized in Discovery Studio version 21.1. Binding affinity scores (kcal/mol) were subjected to principal component analysis (PCA) to cluster phytoconstituents according to interaction patterns. PC1 and PC2 values were derived from the covariance matrix of eigenvectors and eigenvalues.[35] PCA was performed in Minitab version 17.[36] Pharmacophore features of the best docked complexes were analyzed in Discovery Studio version 21.1 using default settings, highlighting steric and electronic features critical for phytoconstituent-protein interactions.

Tetrapartite network and pathway analysis

A tetrapartite network was developed in Cytoscape version 3.9, linking phytoconstituents, best docked protein complexes, protein functions, and pathway proteins.[37] Protein-protein interactions (PPIs) were retrieved using STRING version 12.0 (https://string-db.org/) with a high-confidence score (≥0.70).[38] This approach provides insights into the interactions between phytoconstituents and their target proteins. Metabolic pathways associated with proteins were analyzed using the Kyoto Encyclopedia of Genes and Genomes (KEGG, https://www.genome.jp/kegg/)[39] and the PPI network and visualized in Draw.io version 4.0.

ADME and toxicity analysis

Pharmacokinetic profiles (Absorption, Distribution, Metabolism, and Excretion, ADME) were predicted using SwissADME (http://www.swissadme.ch/),[40] including Lipinski's and Ghose rules, BBB permeability, and bioavailability. Toxicity was evaluated with ProTox-II (https://tox-new.charite.de/protox_II/), predicting carcinogenicity, mutagenicity, and cytotoxicity.[41]

Results and Discussion

Qualitative and quantitative analysis of C. zeylanicum bark *extract*

8.4 g (5.6%) of CzB extract was yielded by methanol extraction, which was used for subsequent analyses. The qualitative analysis confirmed the presence of flavonoids, coumarins, phenols, and quinones in table 2. The TPC, calculated using a gallic acid standard curve ($R^2 = 0.97$), was 43.3 ± 0.27 mg GAE/g extract. The TFC, based on a quercetin standard curve ($R^2 = 0.98$), was 28.93 ± 0.49 mg QE/g extract (figure 1). The significant presence of phenolic and flavonoid compounds suggests that CzB extract is a rich source of these secondary phytoconstituents, contributing to its potential therapeutic applications.

Table 2: Qualitative phytochemical analysis of the extract of *Cinnamomum zeylanicum* bark

S. No.	Phytoconstituents	Result
1	Flavonoid	+
2	Alkaloid	-
3	Coumarin	+
4	Phenol	+
5	Quinone	+

Note: (+) = present, (-) = absent

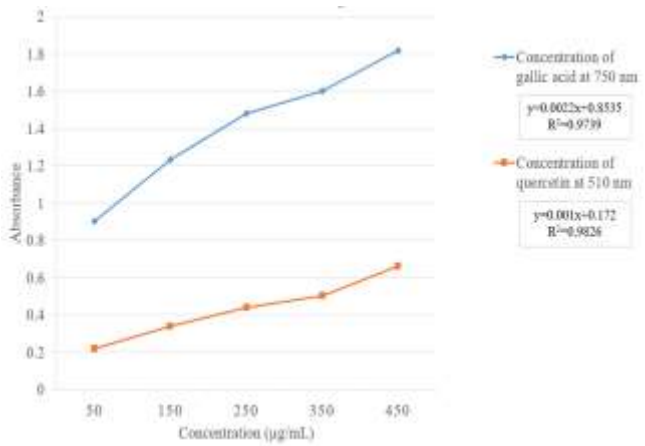

Figure 1: Gallic acid and quercetin calibration graph for estimation of total phenolic content (blue) and total flavonoid content (orange), respectively

GC-MS profiling of phytoconstituents

Nineteen phytoconstituents present in the CzB extract were identified using the GC-MS, as shown in figure 2 and table 3. Cinnamaldehyde was the most abundant constituent (18.37%), followed by (Z)-2-methoxycinnamaldehyde (1.75%). Other phytoconstituents, including α-copaene,[42] coumarin,[43] and τ-cadinol,[44] were also identified, which are recognized for their antibacterial properties. Coumarin is widely reported for its anti-inflammatory and antioxidant properties, which enhance the pharmacological profile of the extract. α-Muurolene has been associated with antimicrobial, anti-inflammatory, and wound-healing activities, in addition to tumor growth inhibition.[45]

Molecular characterization of pathogenic S. aureus

PCR-based identification confirmed the identity and pathogenic potential of *S. aureus* MTCC 96 (figure 3). The 16S rRNA gene of *S. aureus* species confirmed identification, while the detection of virulence genes (plc, nuc, and icaA) indicated a pathogenic profile. The icaA gene encodes polysaccharide intercellular adhesion, which mediates biofilm formation and enhances bacterial resistance to host immune defenses.[46] The plc gene encodes phospholipase C, facilitating tissue invasion through cell membrane disruption.[47] The nuc gene encodes thermonuclease, an enzyme involved in degrading neutrophil extracellular traps, thus aiding immune evasion.[48]

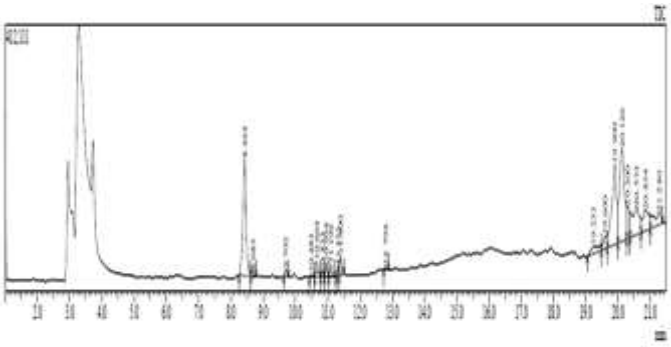

Figure 2: The total ion chromatogram of the GC-MS between intensity and elution time of the *Cinnamomum zeylanicum* bark extract

ISSN 2616-0684 (Print)
ISSN 2616-0692 (Electronic)

Table 3: GC-MS analysis of *Cinnamomum zeylanicum* bark extract with chemical formula and 2D structure

CZ_peak No.	Retention time	Area %	Name of phytoconstituent	Chemical formula	Structure
CZ_1	8.424	18.37	Cinnamaldehyde, (E)-	C_9H_8O	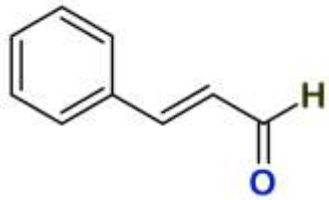
CZ_2	8.683	0.46	Pentadecane	$C_{15}H_{32}$	
CZ_3	9.702	0.61	α-Copaene	$C_{15}H_{24}$	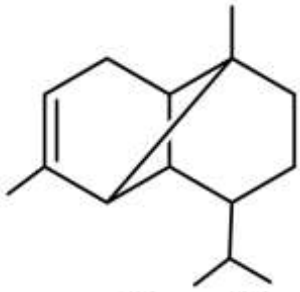
CZ_4	10.483	0.38	Coumarin	$C_9H_6O_2$	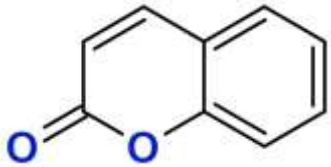
CZ_5	10.664	1.66	Diethyl Phthalate	$C_{12}H_{14}O_4$	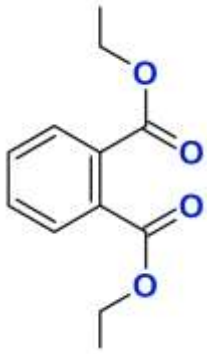
CZ_6	10.833	0.6	(1S,4aR,8aS)-1-Isopropyl-7-methyl-4-methylene-1,2,3,4,4a,5,6,8a-octahydronaphthalene	$C_{15}H_{24}$	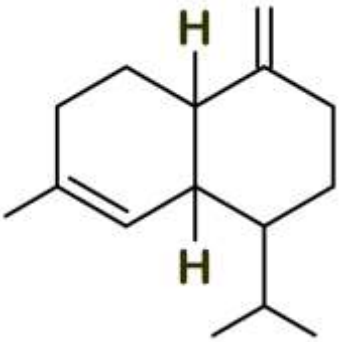
CZ_7	10.954	1.29	Octadecane	$C_{18}H_{38}$	

ISSN 2616-0684 (Print)
ISSN 2616-0692 (Electronic)

CZ_8	11.102	1.17	.α.-Muurolene	$C_{15}H_{24}$	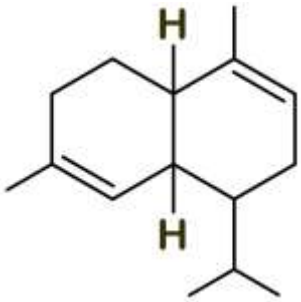
CZ_9	11.321	0.82	Naphthalene, 1,2,4a,5,8,8a-hexahydro-4,7-dimethyl-1-(1-methylethyl)-,[1S-(1.alpha.,4a.beta.,8a.alpha.)]-	$C_{15}H_{24}$	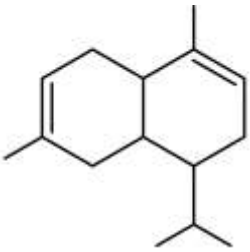
CZ_10	11.4	1.75	(Z)-2-Methoxycinnamaldehyde	$C_{10}H_{10}O_2$	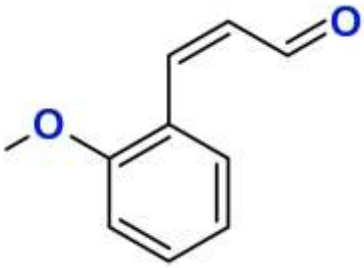
CZ_11	12.794	0.35	τ.-Cadinol	$C_{15}H_{26}O$	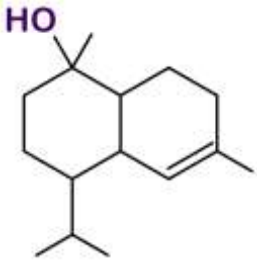
CZ_12	19.233	2.93	1-Heptacosanol	$C_{27}H_{56}O$	
CZ_13	19.6	2.49	Tetracosyl pentafluoropropionate	$C_{31}H_{57}F_5O_2$	
CZ_14	19.9	19.5	Dotriacontane	$C_{32}H_{66}$	
CZ_15	20.126	22.17	Tetracontane	$C_{40}H_{82}$	
CZ_16	20.3	4.57	Tetrapentacontane, 1,54-dibromo-	$C_{54}H_{108}Br_2$	
CZ_17	20.573	9.79	Dotriacontyl pentafluoropropionate	$C_{35}H_{65}F_5O_2$	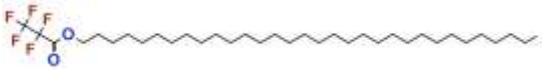

 ISSN 2616-0684 (Print)
ISSN 2616-0692 (Electronic)

CZ_18	20.854	6.26	1-Hexacosanol	$C_{26}H_{54}O$	
CZ_19	21.28	4.82	Sulfurous acid, cyclohexylmethyl heptadecyl ester	$C_{24}H_{48}O_3S$	

Note: CZ = *Cinnamomum zeylanicum.*

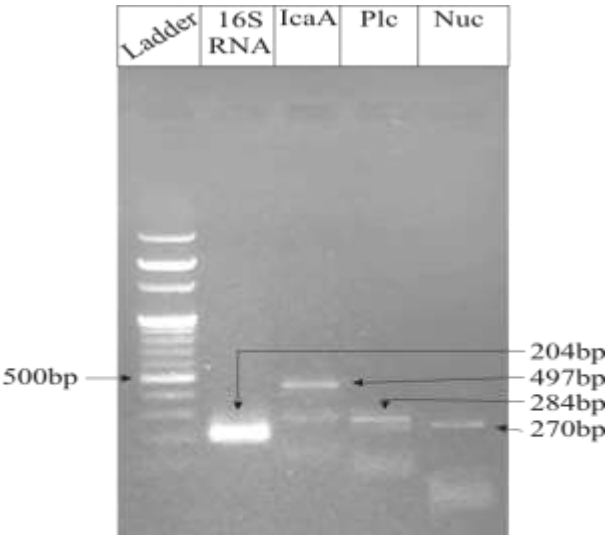

Figure 3: The agarose gel electrophoresis analysis of polymerase chain reaction-amplified genes, with a 100 bp DNA ladder as a reference. The 16S rRNA gene was used for the identification of *Staphylococcus aureus* MTCC96, while the virulence-associated genes include icaA, plc, and nuc

Minimum inhibitory and bactericidal concentration

Bacterial viability was evaluated using a resazurin assay (figure 4). *S. aureus* culture was treated with CzB extract at concentrations ranging from 20 mg/mL to 0.15 mg/mL, with positive (ciprofloxacin) and negative controls. Growth inhibition was observed in wells 1-3, whereas bacteria remained viable from the fourth well onward, indicating an MIC of 5 mg/mL. MBC was determined and confirmed that 5 mg/mL of CzB kills a complete bacterial colony. The MIC and MBC values suggest that the methanol bark extract of *C. zeylanicum* exhibits strong antibacterial activity against *S. aureus*. Previous studies have reported MIC values ranging from 6.25 to 12.5 mg/mL for cinnamon bark extracts against *S. aureus*, depending on the strains.[49,50]

Molecular docking and PCA analysis

The 3D crystal structures of seven target proteins generated via X-ray crystallography were retrieved from the PDB with high resolution (≤2 Å). Protein quality was checked using ProCheck, ERRAT (>90% quality), and Verify3D for sequence-structure compatibility. Active site and grid parameters are predicted by Discovery Studio and the Autodock tool, given in table 4. The molecular docking approach was conducted on target proteins and 19 phytoconstituents. PCA was done using the binding affinity score of the docked target protein-ligand complex, where the calculated eigenvalue of the correlation matrix is 5.45 and creates four clusters shown in figure 5b. Phytoconstituents present in clusters 3 and 4 showed strong negative binding affinities with target proteins. Heatmap and PCA screened eight phytoconstituents (CZ_3, CZ_4, CZ_5, CZ_6, CZ_8, CZ_9, CZ_10, and CZ_11) that strongly interact with four target proteins, including peptide deformylase (PDF, 6JFG), D-alanine-D-alanine ligase (DDL, 2I8C), dihydrofolate reductase (DHFR, 4TU5), and penicillin-binding protein 2a (PBP, 5M19), shown in figure 5a. CZ_3 (α-copaene) interacted with 2I8C and 4TU5, having -7.1 kcal/mol binding affinity. CZ_4 (coumarin) exhibited -6.5 and -6.4 kcal/mol binding affinity with 4TU5 and 6JFG, respectively, and CZ_5 (diethyl phthalate) also showed a binding affinity of -6.3 kcal/mol with both proteins 4TU5 and 6JFG. CZ_6 ((1S,4aR,8aS)-1-Isopropyl-7-methyl-4-methylene-1,2,3,4,4a,5,6,8a-octahydronaphtha) displayed -6.8 kcal/mol and -6.6 kcal/mol, and CZ_8 (α-muurolene) demonstrated -7.7 kcal/mol and -7.0 kcal/mol with 4TU5 and 2I8C, respectively. CZ_9 (naphthalene, 1,2,4a,5,8,8a-hexahydro-4,7-dimethyl-1-(1-methylethyl)-,[1S-(1.alpha)]) showed -7.6 kcal/mol, -7.0 kcal/mol, and -7.0 kcal/mol with 4TU5, 2I8C, and 6JFG, respectively. CZ_10 ((Z)-2-Methoxycinnamaldehyde) exhibited -6.5 kcal/mol with 4TU5. CZ_11 (τ-cadinol) showed -7.2 kcal/mol, -6.9 kcal/mol, and -6.2 kcal/mol with 6JFG, 2I8C, and 5M19, respectively. All binding affinity scores of molecular docking analysis are given in supplementary table. Based on the binding affinity score and PCA analysis, CZ_3, CZ_8, CZ_9, and CZ_11 showed higher binding interactions with target proteins, including 2I8C, 4TU5, 6JFG, and 5M19, which were subject to further analysis.

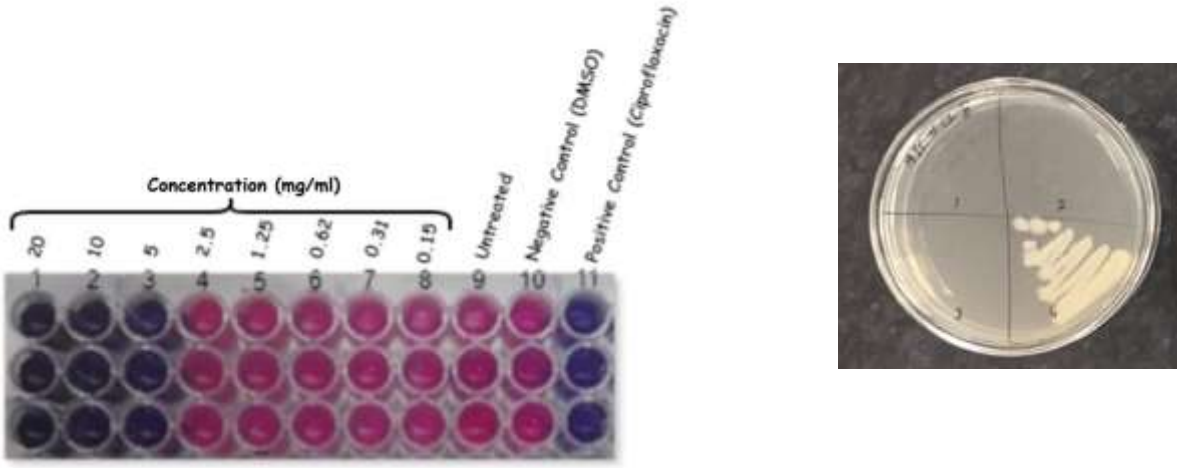

Figure 4: The results of the (a) minimum inhibitory concentration and (b) minimum bactericidal concentration of the extract of *Cinnamomum zeylanicum* bark on *Staphylococcus aureus* MTCC96

 ISSN 2616-0684 (Print)
ISSN 2616-0692 (Electronic)

Table 4: Seven target proteins of *Staphylococcus aureus* with their center grid parameter, dimensions, and ProCheck, ERRAT, and Verified 3D results

PDB ID	1LJL	5M19	6JFG	1SFJ	2I8C	1QXZ	4TU5
Target proteins name	Arsenate reductase (AR)	Penicillin-binding protein 2a (PBPs)	Peptide deformylase (PDF)	3-dehydroquinate dehydratase (DHQD)	D-alanine-D-alanine ligase (DDL)	Methionine aminopeptidase (MAP)	Dihydrofolate reductase (DHFR)
Center grid box (X, Y, Z)	17.17, −3.62, 36.91	−20.65, −17.8, 51.81	−31.38, 22.41, 2.88	104.97, −17.41, −107.42	7.96, −13.99, 10.42	12.33, 4.01, 1.74	−1.25, 34.66, 5.46
Dimension point (Å) (X, Y, Z)	24, 30, 26	28, 22, 22	36, 48, 64	38, 60, 48	66, 68, 76	46, 54, 42	84, 74, 66
ProCheck (favored regions %)	95.6	90.9	93.1	91.5	90.7	94.1	90.4
ERRAT (%)	94.262	95.132	91.819	94.582	92.814	93.724	98.592
Verify 3D (%)	Pass (100%)	Pass (95.76%)	Pass (97.27%)	Pass (83.7%)	Pass (90.46%)	Pass (97.98%)	Pass (84.71%)

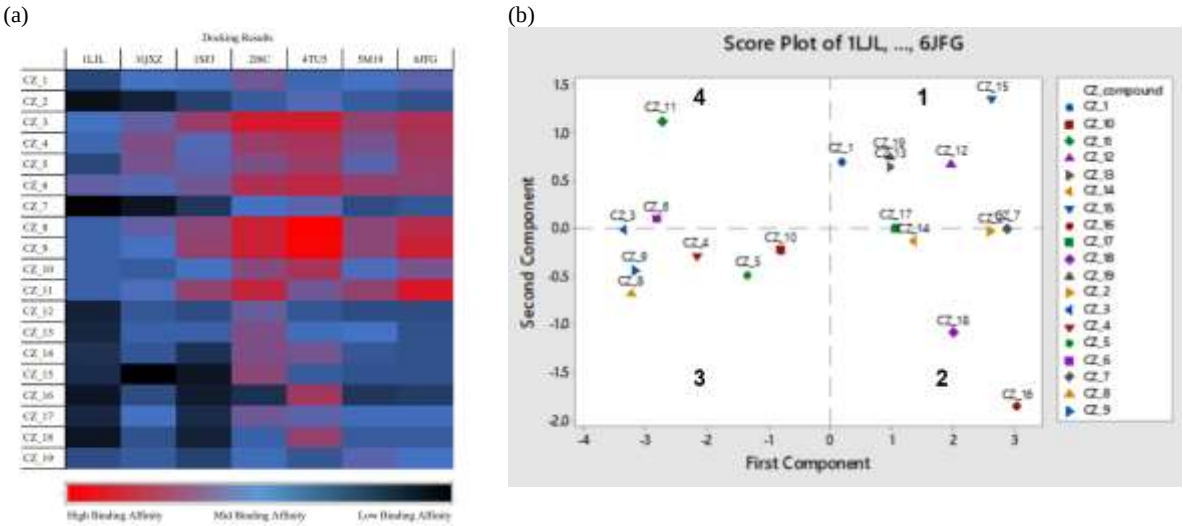

Figure 5: Heatmap and Principal Component Analysis (PCA) of the molecular docking score. (a) Heatmap of molecular docking showing the highest binding affinity of seven target proteins with phytoconstituents. (b) PCA graph representing four different clusters that represent the phytoconstituents

Pharmacophore and docked complexes interaction analysis

Pharmacophore modeling of phytoconstituents revealed hydrophobic interaction properties, which were the main contributors to binding for CZ_3 and CZ_8 with the target protein, whereas CZ_11 gained additional strength through having hydrogen bonding capacity, as shown in figure 6. CZ_3 contains two aromatic rings linked to a methyl group, which increases hydrophobicity and facilitates alkyl bonds. It interacts with amino acids VAL59, VAL121, LEU122, ALA125, and MET128 with 6JFG; amino acids LEU20, ILE14, and VAL6 with 2I8C; ARG241 and VAL277 with 4TU5; and HIS293 with 5M19. CZ_8 and CZ_9 are isomers, so both phytoconstituents displayed similar interactions with target proteins. CZ_8 interacted through hydrophobic regions as well as, due to its steric configuration, formed alkyl and π-alkyl bonds involving amino acids VAL59, LEU112, CYS111, HIS154, VAL151, LEU105, TYR147, and ALA244 with 6JFG; PHE175, PHE295, LEU145, VAL216, and ILE14 with 2I8C; VAL31, LEU5, PHE92, and HIS293 with 4TU5; and VAL277, VAL256, and ARG241 with 5M19. CZ_11 is the hydroxylated form of CZ_8, which gains additional pharmacophore properties of hydrogen bonding formation. Its OH group acted as a donor, forming two hydrogen bonds with VAL59 and GLY60 and alkyl bonds with HIS154, LEU105, TYR147, and VAL151 with 6JFG. It also formed an alkyl bond using LYS348 and a hydrogen bond using PHE206 with 2I8C, alkyl and π-alkyl bonds with LYS33, LEU34, PHE151, HIS30, and VAL137 with 4TU5, and a hydrogen bond using GLU239 along with alkyl bonds involving VAL277, ARG151, VAL256, ARG241, HIS293, and MET372 with 5M19. These findings suggest that binding interaction capabilities of CzB phytoconstituents and slight structural modifications of these phytoconstituents, particularly hydroxylation, could enhance their drug-like properties.

ISSN 2616-0684 (Print)
ISSN 2616-0692 (Electronic)

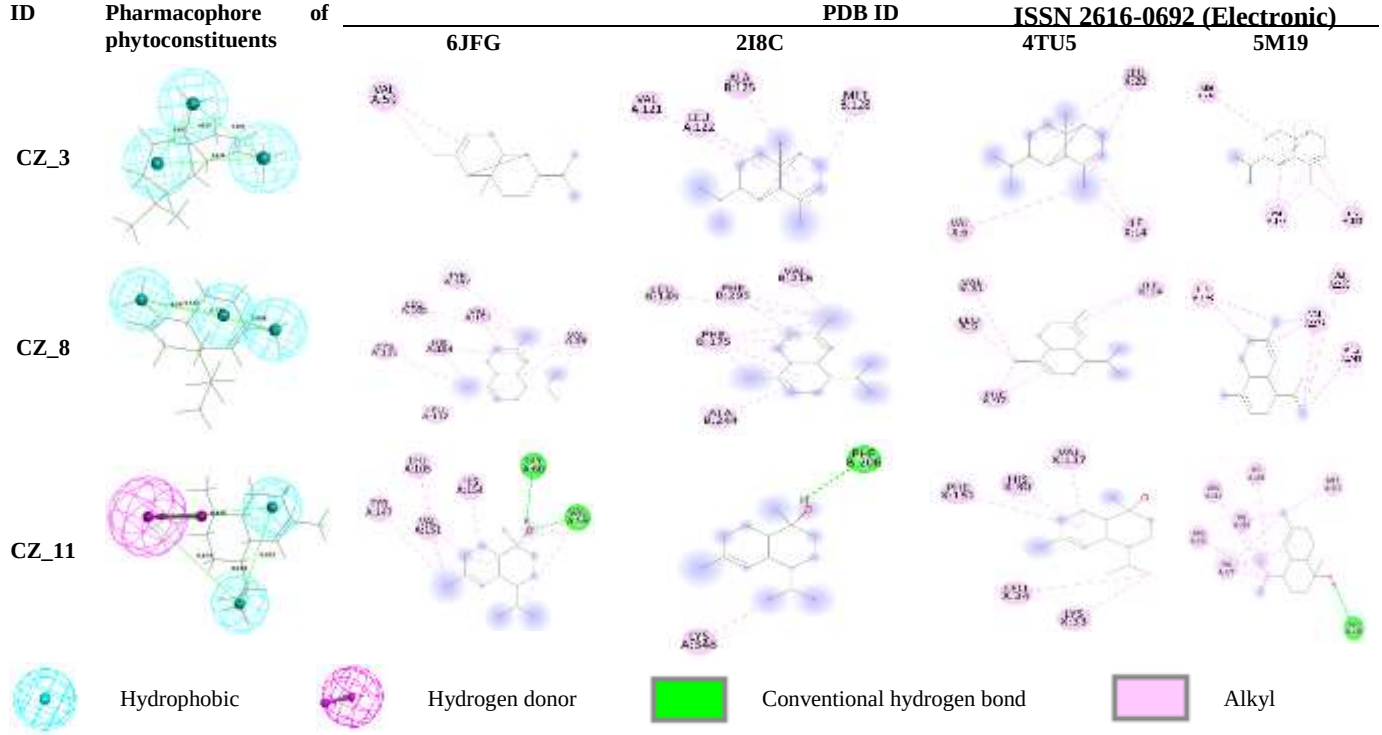

Figure 6: The pharmacophore properties of the phytoconstituents and interactions between the target proteins of *Staphylococcus aureus* and phytoconstituents

Tetrapartite network and pathway analysis

The PPIs network of target proteins of *S. aureus*, including phytoconstituents, facilitates an understanding of the molecular function of key proteins, their associated proteins, and interacting phytoconstituents, as illustrated in figure 7. Eight CzB phytoconstituents exhibited the most significant interactions with four key target proteins: 5M19, 2I8C, 4TU5, and 6JFG. The target proteins 5M19 and 2I8C contribute functional roles in cell wall biosynthesis, while 4TU5 and 6JFG are essential in nucleotide synthesis and translation. Further, STRING analysis revealed that PBP-3 (ABD30728.1) and PBP-1 (ABD30255.1) are linked to 5M19, while 2I8C is connected with Mur family proteins. Additionally, 4TU5 connects to thymidylate synthase, critical for DNA replication, and 6JFG is associated with ribosomal proteins (rplU, tig, rplV, rplS, and map).

The metabolic pathway of target proteins was reconstructed and connected with associated proteins on the basis of KEGG pathway analysis, as presented in figure 8.[39] PBP2a and DDL were integrated within the peptidoglycan biosynthesis pathway, which is essential for bacterial survival and β-lactam resistance. MecA protein has a role in the synthesis of PBPs. The metabolism of amino acids, nucleotide sugars, and D-amino acid metabolism pathways contributes to the synthesis of Mur family proteins (MurB, MurC, and MurF) and D-ala-D-ala, respectively. D-ala-D-ala is linked to enhance the function of PBPs. Purine, phenylalanine, and pterin biosynthesis pathways are involved in the formation of tetrahydrofolate and dihydrofolate synthase. These findings demonstrate that *C. zeylanicum* phytoconstituents act on multiple target proteins, which can interfere with cell wall integrity and nucleic acid metabolism.

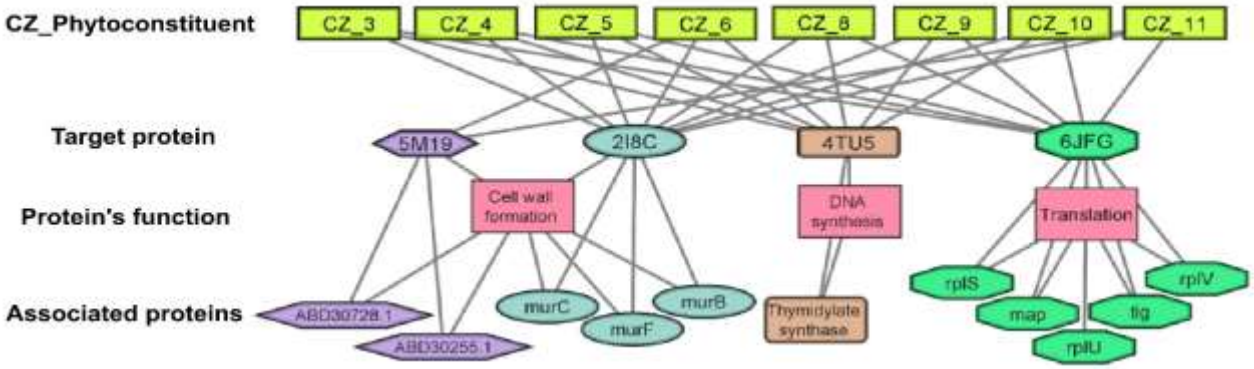

Figure 7: A tetrapartite network illustrates the interactions between *Cinnamomum zeylanicum* bark phytoconstituents and their target proteins, along with the protein functions and their linkages to associated proteins

 ISSN 2616-0684 (Print)
ISSN 2616-0692 (Electronic)

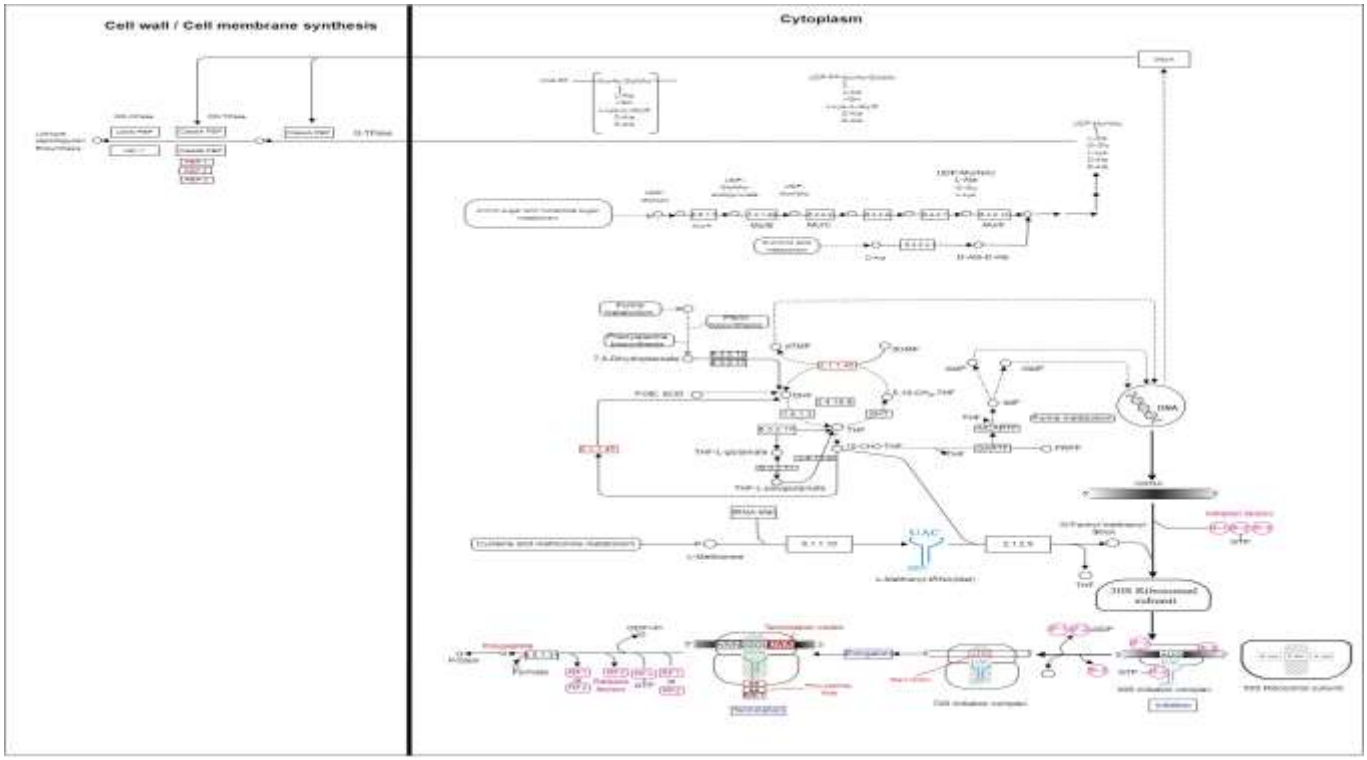

Figure 8: The illustration of metabolic pathways including four target proteins: D-alanine-D-alanine ligase, dihydrofolate reductase, peptide deformylase, and penicillin-binding protein in *Staphylococcus aureus*.[39] The highlighted color illustrates the distinct metabolic pathways associated with each of these target proteins

ADME and toxicity analysis

ADME analysis provides insights into the body's response to administered phytoconstituents, given in table 5. Nineteen phytoconstituents were evaluated for BBB permeability, Lipinski's and Ghose rule violations, and bioavailability. The BBB regulates exchange between circulating blood and the brain's extracellular fluid.[51] Six phytoconstituents (CZ_1, CZ_3, CZ_4, CZ_5, CZ_10, and CZ_11) showed BBB permeability. Evaluation of drug-likeness using Lipinski's Rule of Five and the Ghose Rule revealed that CZ_5, CZ_10, and CZ_11 met both criteria, while CZ_3, CZ_8, and CZ_9 violated only one Lipinski rule but satisfied the Ghose Rule, suggesting acceptable pharmacokinetic potential. Seven phytoconstituents (CZ_3, CZ_5, CZ_6, CZ_8, CZ_9, CZ_10, and CZ_11) exhibited a bioavailability score of 0.55, indicating favorable oral absorption.

Toxicity predictions using ProTox 3.0 showed no hepatotoxicity among the phytoconstituents. However, CZ_4, CZ_10, CZ_11, CZ_13, CZ_16, and CZ_17 were associated with carcinogenic potential, CZ_6 and CZ_9 with immunotoxicity, and CZ_4 with cytotoxicity. Additionally, CZ_1, CZ_10, CZ_11, and CZ_16 displayed mutagenic activity, while CZ_3 and CZ_8 were non-toxic as the most promising leads, balancing efficacy with safety.

Table 5: The ADME (Absorption, Distribution, Metabolism, and Excretion) and toxicity profile of phytoconstituents of *Cinnamomum zeylanicum* bark

CZ_ID	ADME				Toxicity				
	BBB permeate	Lipinski violations	Ghose violations	Bioavailability Score	Hepatotoxicity	Carcinogenicity	Immunotoxicity	Cytotoxicity	Mutagenicity
CZ_1	Yes	0	2	0.55	Inactive	Inactive	Inactive	Inactive	Active
CZ_2	No	1	4	0.55	Inactive	Inactive	Inactive	Inactive	Inactive
CZ_3	Yes	1	0	0.55	Inactive	Inactive	Inactive	Inactive	Inactive
CZ_4	Yes	0	2	0.55	Inactive	Active	Inactive	Active	Inactive
CZ_5	Yes	0	0	0.55	Inactive	Inactive	Inactive	Inactive	Inactive
CZ_6	No	1	0	0.55	Inactive	Inactive	Active	Inactive	Inactive
CZ_7	No	1	1	0.55	Inactive	Inactive	Inactive	Inactive	Inactive
CZ_8	No	1	0	0.55	Inactive	Inactive	Inactive	Inactive	Inactive
CZ_9	No	1	0	0.55	Inactive	Inactive	Active	Inactive	Inactive
CZ_10	Yes	0	0	0.55	Inactive	Active	Inactive	Inactive	Active
CZ_11	Yes	0	0	0.55	Inactive	Active	Inactive	Inactive	Active

ISSN 2616-0684 (Print)
ISSN 2616-0692 (Electronic)

CZ_12	No	1	3	0.55	Inactive	Inactive	Inactive	Inactive	Inactive
CZ_13	No	2	4	0.17	Inactive	Active	Inactive	Inactive	Inactive
CZ_14	No	1	3	0.55	Inactive	Inactive	Inactive	Inactive	Inactive
CZ_15	No	2	4	0.17	Inactive	Inactive	Inactive	Inactive	Inactive
CZ_16	No	2	4	0.17	Inactive	Active	Inactive	Inactive	Active
CZ_17	No	2	4	0.17	Inactive	Active	Inactive	Inactive	Inactive
CZ_18	No	1	2	0.55	Inactive	Inactive	Inactive	Inactive	Inactive
CZ_19	No	1	2	0.55	Inactive	Inactive	Inactive	Inactive	Inactive

Note: ADME = Absorption, Distribution, Metabolism, and Excretion, CZ = *Cinnamomum zeylanicum*, BBB permeate = Blood-Brain Barrier permeability.

Conclusion

The phytoconstituents, including α-copaene, α-muurolene, and τ-cadinol, present in *C. zeylanicum* bark exhibit antibacterial potential against pathogenic *S. aureus*. The primary target proteins include D-alanine-D-alanine ligase, dihydrofolate reductase, peptide deformylase, and penicillin-binding protein 2a, indicating disruption of cell wall formation, nucleic acid metabolism, and protein synthesis. Multi-target suggests a synergistic antibacterial mechanism that may reduce the risk of resistance. Future investigations should focus on the purification and fractionation of identified phytoconstituents, followed by *in vitro* and *in vivo* validation. Structure optimization may further improve their potency and safety, supporting their development as promising natural anti-*S. aureus* therapeutics.

Conflict of interest

The authors declare no conflict of interest.

Authors' Declaration

The authors hereby declare that the work presented in this article is original, and any liability for claims relating to the content of this article will be borne by them.

Acknowledgments

The authors gratefully acknowledge Maulana Azad National Institute of Technology, Bhopal, India, for providing the research facilities. We extend our sincere thanks to Dr. Bharat K Modhera and Mr. Jamna P Gujar for their assistance with GC-MS analysis at the Department of Chemical Engineering. We also thank the Central Computing Facility for providing access to HPC resources.

References

1. Kumar, N.R., Balraj, T.A., Kempegowda, S.N., and Prashant, A. Multidrug-Resistant Sepsis: A Critical Healthcare Challenge. Antibiotics. 2024;13(1):46. doi: 10.3390/antibiotics13010046
2. Patel, H., and Rawat, S. A genetic regulatory see-saw of biofilm and virulence in MRSA pathogenesis. Front Microbiol. 2023;14:1204428. doi: 10.3389/fmicb.2023.1204428
3. Rai, A., and Khairnar, K. Overview of the risks of *Staphylococcus aureus* infections and their control by bacteriophages and bacteriophage-encoded products. Brazilian J Microbiol. 2021;52(4):2031–2042. doi: 10.1007/s42770-021-00566-4
4. Haindongo, E.H., Ndakolo, D., Hedimbi, M., Vainio, O., Hakanen, A., and Vuopio, J. Antimicrobial resistance prevalence of *Escherichia coli* and *Staphylococcus aureus* amongst bacteremic patients in Africa: a systematic review. J of Glob Antimicrob Resist. 2023;32:35–43. doi: 10.1016/j.jgar.2022.11.016
5. Eltwisy, H.O., Twisy, H.O., Hafez, M.H.R., Sayed, I.M., and El-Mokhtar, M.A. Clinical Infections, Antibiotic Resistance, and Pathogenesis of *Staphylococcus haemolyticus*. Microorganisms. 2022;10:1130. doi: 10.3390/microorganisms10061130
6. Zhu, Z., Hu, Z., Li, S., Fang, R., Ono, H.K., and Hu, D.L. Molecular Characteristics and Pathogenicity of *Staphylococcus aureus* Exotoxins. Int J Mol Sci. 2024;25(1):395. doi: 10.3390/ijms25010395
7. Yu, J., Jiang, F., Zhang, F., Hamushan, M., Du, J., Mao, Y., Wang, Q., and Shen, H. Thermonucleases contribute to *Staphylococcus aureus* biofilm formation in implant-associated infections–A redundant and complementary story. Front Microbiol. 2021;12:687888. doi: 10.3389/fmicb.2021.687888
8. Yu, J., Han, W., Xu, Y., Shen, L., Zhao, H., Zhang, J., Xiao, Y., Guo, Y., and Yu, F. Biofilm-producing ability of methicillin-resistant *Staphylococcus aureus* clinically isolated in China. BMC Microbiol. 2024;24(1):241. doi: 10.1186/s12866-024-03380-8
9. Singh, I., Roshan, M., Vats, A., Behera, M., Gautam, D., Rajput, S., Rana, C., and De, S. Evaluation of Virulence, Antimicrobial Resistance and Biofilm Forming Potential of Methicillin-Resistant *Staphylococcus aureus* (MRSA) Isolates from Bovine Suspected with Mastitis. Curr Microbiol. 2023;80(6):198. doi: 10.1007/s00284-023-03303-2
10. Hou, Z., Liu, L., Wei, J., and Xu, B. Progress in the Prevalence, Classification and Drug Resistance Mechanisms of Methicillin-Resistant *Staphylococcus aureus*. Infect Drug Resist. 2023;16:3271–3292. doi: 10.2147/IDR.S412308
11. Gu, D.T., Tung, T.H., Jiesisibieke, Z.L., Chien, C.W., and Liu, W.Y. Safety of Cinnamon: An Umbrella Review of Meta-Analyses and Systematic Reviews of Randomized Clinical Trials. Front Pharmacol. 2022;12(18):790901. doi: 10.3389/fphar.2021.790901
12. Ribeiro-santos, R., Andrade, M., Madella, D., Melo, D., Paula, A., Aquino, L. De, Moura, G., and Sanches-silva, A. Revisiting an ancient spice with medicinal purposes: Cinnamon. Trends Food Sci Technol. 2017;62:154–169. doi: 10.1016/j.tifs.2017.02.011
13. Khalisyaseen, O., and Mohammed, M.T. Analytics Detection of Phytochemical Compounds in *Cinnamomum zeylanicum* Bark Extract. Egypt J Chem. 2023;66(4):265–273. doi: 10.21608/EJCHEM.2022.146416.6366
14. Prabhashini, W., Mendis, K., Arachchige, G., and Premakumara, S. Anti-inflammatory, cytotoxicity and antilipidemic properties : novel bioactivities of true cinnamon (*Cinnamomum zeylanicum* Blume) leaf. BMC Complement Med Ther. 2022;22:259. doi: 10.1186/s12906-022-03728-5

15. Alizadeh Behbahani, B., Falah, F., Lavi Arab, F., Vasiee, M., and Tabatabaee Yazdi, F. Chemical Composition and Antioxidant, Antimicrobial, and Antiproliferative Activities of *Cinnamomum zeylanicum* Bark Essential Oil. J Evid Based Complement Altern Med. 2020;2020:1590603. doi: 10.1155/2020/5190603
16. Nawaz, A., Ali, T., Naeem, M., Hussain, F., Li, Z., and Nasir, A. Biochemical, structural characterization and in-vitro evaluation of antioxidant, antibacterial, cytotoxic, and antidiabetic activities of nanosuspensions of *Cinnamomum zeylanicum* bark extract. Front Chem. 2023;11:1194389. doi: 10.3389/fchem.2023.1194389
17. Quyen, P.T., and Quoc, L.P.T. Chemical Profile and Biological Activities of The Essential Oil of Cinnamon (*Cinnamomum cassia* (L.) J. Presl) Twigs and Leaves. Trop J Nat Prod Res. 2023;7(11):5226–5230. doi: 10.26538/tjnpr/v7i11.29
18. Rollando, R., Eva, M., Dodi, I., Viol, D.K., and Arif, N.M. *Goniothalamus macrophyllus*: A Comprehensive Review of Its Phytochemistry, Pharmacological Activities, and Therapeutic Potential. Trop J Nat Prod Res. 2025;7(9):2964–2972. doi: 10.26538/tjnpr/v9i7.3
19. Mulpuru, V., and Mishra, N. Computational Identification of SARS-CoV-2 Inhibitor in *Tinospora cordifolia*, *Cinnamomum zeylanicum* and *Myristica fragrans*. VirusDisease. 2021;32(3):511–517. doi: 10.1007/s13337-021-00721-3
20. Meylani, V., Rizal Putra, R., Miftahussurur, M., Sukardiman, S., Eko Hermanto, F., and Abdullah, A. Molecular docking analysis of *Cinnamomum zeylanicum* phytochemicals against Secreted Aspartyl Proteinase 4–6 of *Candida albicans* as anti-candidiasis oral. Results Chem. 2023;5:100721. doi: 10.1016/j.rechem.2022.100721
21. Pourkhosravani, E., Nayeri, F.D., and Bazargani, M.M. Decoding antibacterial and antibiofilm properties of cinnamon and cardamom essential oils : a combined molecular docking and experimental study. AMB Express. 2021;11:143. doi: 10.1186/s13568-021-01305-6
22. Julianti, E., Rajah, K.K., and Fidrianny, I. Antibacterial activity of ethanolic extract of Cinnamon bark, honey, and their combination effects against acne-causing bacteria. Sci Pharm. 2017;85(2):19. doi: 10.3390/scipharm85020019
23. Mujeeb, F., Bajpai, P., and Pathak, N. Phytochemical Evaluation, Antimicrobial Activity, and Determination of Bioactive Components from Leaves of *Aegle marmelos*. BioMed Res Int. 2014;2014:497606. doi: 10.1155/2014/497606
24. Dvorackova, E., Snoblova, M., Chromcova, L., and Hrdlicka, P. Effects of extraction methods on the phenolic compounds contents and antioxidant capacities of cinnamon extracts. Food Sci Biotechnol. 2015;24(4):1201–1207. doi: 10.1007/s10068-015-0154-4
25. Rugaie, O. Al, Mohammed, H.A., Alsamani, S., Messaoudi, S., Aroua, L.M., Khan, R.A., Almahmoud, S.A., and Altaleb, A.D. Antimicrobial , Antibiofilm , and Antioxidant Potentials of Four Qassim Region of Saudi Arabia : Phytochemical Profile and In Vitro and In Silico Bioactivity Investigations. Antibiotics. 2023;12(3):501. doi: 10.3390/antibiotics12030501
26. Rhetso, T., Seshadri, R.M., Ramnath, S., and Venkataramegowda, S. GC-MS based metabolite profiling and antioxidant activity of solvent extracts of *Allium Chinense* G Don leaves. Not Sci Biol. 2021;13(2):10791. doi: 10.15835/nsb13210791
27. Precious, A.I., Joan, M.O., David, A.Z., Fatima, A.S., Ummulkhairi, T., Endaline, A.M., Obumneme. C.O., Abubakar, R.M., and Samson, C.O. Antidiabetic Activity and in silico Molecular Docking of GC-MS-Identified Compounds in Chromatographic Fractions of *Tephrosia bracteolata* Guill. & Perr.(Fabaceae) Leaves. Trop J Nat Prod Res. 2025;9(8):3720–3728. doi: 10.26538/tjnpr/v9i8.31
28. Brakstad, O.D.D.G., Aasbakk, K., and Maeland, J.A. Detection of *Staphylococcus aureus*_nuc pcr und primer. J Clin microbiol. 1992;30(7):1654–1660. doi: 10.1128/jcm.30.7.1654-1660.1992
29. Mith, H., Duré, R., Delcenserie, V., Zhiri, A., Daube, G., and Clinquart, A. Antimicrobial activities of commercial essential oils and their components against food-borne pathogens and food spoilage bacteria. Food Sci Nutr. 2014;2(4):403–416. doi: 10.1002/fsn3.116
30. Prabha, S., Chauhan, P., Warkare, S., and Pandey, K.M. A computational investigation of potential plant-based bioactive compounds against drug-resistant *Staphylococcus aureus* of multiple target proteins. J Biomol Struct Dyn. 2023;43(7):3311–3329. doi: 10.1080/07391102.2023.2297009
31. Kirchmair, J., Markt, P., Distinto, S., Schuster, D., Spitzer, G.M., Liedl, K.R., Langer, T., and Wolber, G. The Protein Data Bank (PDB), Its Related Services and Software Tools as Key Components for In Silico Guided Drug Discovery. J Med Chem. 2008;51(22):7021–7040. doi: 10.1021/jm8005977
32. Trott, O., and Olson, A.J. AutoDock Vina: improving the speed and accuracy of docking with a new scoring function, efficient optimization and multithreading. J Comput Chem. 2010;31(1):455–461. doi: 10.1002/jcc.21334
33. Csizmadia, P. MarvinSketch and MarvinView: Molecule Applets for the World Wide Web, in Proceedings of the 3rd International Electronic Conference on Synthetic Organic Chemistry. MDPI:Basel, Swit. 1999. doi: 10.3390/ecsoc-3-01775
34. Boyle, N.M.O., Banck, M., James, C.A., Morley, C., Vandermeersch, T., and Hutchison, G.R. Open Babel : An open chemical toolbox. J Cheminform. 2011;3:33. doi: 10.1186/1758-2946-3-33
35. Maćkiewicz, A., and Ratajczak, W. Principal components analysis (PCA). Computers & Geosciences. 1993;19(3):303–342. doi: 10.1016/0098-3004(93)90090-R
36. Alin, A. Minitab. WIREs Comput Stat. 2010;2(6):723–727. doi: 10.1002/wics.113
37. Kohl, M., Wiese, S., and Warscheid, B. Cytoscape: Software for Visualization and Analysis of Biological Networks. In: Hamacher, M., Eisenacher, M., Stephan, C. (eds) Data Mining in Proteomics. Methods Mol Bio. 2011;696. doi: 10.1007/978-1-60761-987-1_18
38. Szklarczyk, D., Franceschini, A., Kuhn, M., Simonovic, M., Roth, A., Minguez, P., Doerks, T., Stark, M., Muller, J., Bork, P., Jensen, L.J., and Mering, C. von. The STRING database in 2011: functional interaction networks of proteins, globally integrated and scored. Nucl Acids Res. 2010;39(suppl_1):D561–D568. doi: 10.1093/nar/gkq973
39. Aoki, K.F., and Kanehisa, M. Using the KEGG Database Resource. Current Protocols in Bioinforma. 2005;11:1.12.1-1.12.54. doi: 10.1002/0471250953.bi0112s11
40. Daina, A., Michielin, O., and Zoete, V. SwissADME : a free web tool to evaluate pharmacokinetics , drug- likeness and medicinal chemistry friendliness of small molecules. Sci Rep. 2017;7:42717. doi: 10.1038/srep42717
41. Banerjee, P., Eckert, A.O., Schrey, A.K., and Preissner, R. ProTox-II: a webserver for the prediction of toxicity of chemicals. Nucl Acids Res. 2018;46(W1):W257–W263. doi: 10.1093/nar/gky318
42. Lang, G., and Buchbauer, G. A review on recent research results (2008–2010) on essential oils as antimicrobials and antifungals. A review. Flavour Fragr J. 2012;27(1):13–39. doi: 10.1002/ffj.2082
43. 43. Ranjan Sahoo, C., Sahoo, J., Mahapatra, M., Lenka, D., Kumar Sahu, P., Dehury, B., Nath Padhy, R., and Kumar Paidesetty, S. Coumarin derivatives as promising

ISSN 2616-0684 (Print)
ISSN 2616-0692 (Electronic)

antibacterial agent(s). Arab J Chem. 2021;14(2):102922. doi: 10.1016/j.arabjc.2020.102922

44. Santos, A.L. dos, Amaral, M., Hasegawa, F.R., Lago, J.H.G., Tempone, A.G., and Sartorelli, P. (-)-T-Cadinol—a Sesquiterpene Isolated From *Casearia sylvestris* (Salicaceae)—Displayed In Vitro Activity and Causes Hyperpolarization of the Membrane Potential of *Trypanosoma cruzi*. Front Pharmacol. 2021;12:734127. doi: 10.3389/fphar.2021.734127
45. Komane, B., Kamatou, G., Mulaudzi, N., Vermaak, I., and Fouche, G. Chapter 21 - Sclerocarya birrea. The south Afri herb Pharmacopoeia. 2023:471-501. doi: 10.1016/B978-0-323-99794-2.00027-1
46. Abdel-Shafi, S., El-Serwy, H., El-Zawahry, Y., Zaki, M., Sitohy, B., and Sitohy, M. The Association between icaA and icaB Genes, Antibiotic Resistance and Biofilm Formation in Clinical Isolates of Staphylococci spp. Antibiotics. 2022;11(3):389. doi: 10.3390/antibiotics11030389
47. Nakamura, Y., Kanemaru, K., Shoji, M., Totoki, K., Nakamura, K., Nakaminami, H, Nakase K, Noguchi N & Fukami K. Phosphatidylinositol-specific phospholipase C enhances epidermal penetration by *Staphylococcus aureus*. Sci Rep. 2020;10:17845. doi: 10.1038/s41598-020-74692-8
48. Kiedrowski, M.R., Crosby, H.A., Hernandez, F.J., Malone, C.L., McNamara, J.O., and Horswill, A.R. *Staphylococcus aureus* Nuc2 is a functional, surface-attached extracellular nuclease. PLoS ONE. 2014;9(4):e95574. doi: 10.1371/journal.pone.0095574
49. Devara, M.S., Bhamidipati, S., Dondapati, V.B., and Bandaru, N.R. Antibacterial activity of cinnamon extract against gram-positive and gram-negative bacterial pathogens isolated from patient samples. Med. Lab. J. 2023;17(6):1–3. doi: 10.61186/mlj.17.6.1
50. Tamiru T, D.T., and Belete D, B.B. Antimicrobial Potentials of Apis Multiflora Honey in Combination with Coffee and Cinnamon Extracts against Common Human Pathogenic Bacteria. Med. Aromat. Plant. 2015;4(4):208. doi: 10.4172/2167-0412.1000208
51. Shaker, B., Yu, M.S., Song, J.S., Ahn, S., Ryu, J.Y., Oh, K.S., Na, Dokyun. LightBBB: Computational prediction model of blood-brain-barrier penetration based on LightGBM. Bioinformatics. 2021;37(8):1135–1139. doi: 10.1093/bioinformatics/btaa918